Does exchange produce L dependence in the optical model potential?

D. Lukaszek and G. H. Rawitscher
Physics Department, University of Connecticut, Storrs, Connecticut 06268
(Received 7 February 1994)

We obtain a local but angular momentum dependent potential V_L which is phase equivalent to a Hartree-Fock nonlocal potential for the description of nucleon-nucleus scattering. We first identify two different pieces of the microscopic effective nucleon-nucleon interaction, guided by an analysis of the L-dependent properties of the conventional microscopic direct and exchange matrix elements of the n-n interaction. By separately folding these two pieces of the effective n-n interaction over the nucleons in the target nucleus we obtain two different microscopic local potentials. We finally obtain V_L from the superposition of these two potentials with L-dependent coefficients, determined such that the deviation of the scattering wave function from the exact solution of the nonlocal Schrödinger equation, with the Hartree-Fock potential, is as small as possible. We provide a numerical example for n-^{16}O scattering at 20 and 50 MeV. We find that the deviation of the wave functions for V_L is only a little smaller than the deviation for a local L-independent potential obtained by inversion of the scattering phase shifts. Hence the latter provides a nearly optimum local description of the exchange nonlocality.

PACS number(s): 24.10.Ht, 25.40.Dn

I. INTRODUCTION

In nucleon-nucleus scattering the exchange part of the interaction (due to the Pauli exclusion principle) contributes substantially to the overall optical potential. For the scattering of neutrons from the nucleus of oxygen at 20 and 50 MeV, the exchange contribution is nearly half of the total [1]. Since the exchange (or Fock) part of the optical model is nonlocal, and hence gives rise to angular-momentum- (L-) dependent effects, it is surprising that local L-independent optical potentials do so well in describing elastic-scattering cross sections and polarization asymmetries.

There is some evidence that the optical-model potential should be L dependent. A careful study of the n-^{208}Pb cross sections at low energies [2] suggested that an L dependence of the imaginary part of the optical potential would be desirable. In two subsequent studies [3,4] of the validity of the dispersion relation constrained optical potential for n-^{208}Pb scattering it was again found that an L-dependent imaginary potential W was desirable so as to make the extension to negative energies more uniformly feasible. Because of the dispersion relations, the real part of the optical potential deviates from a conventional Woods-Saxon shape in an L-dependent fashion also. In an additional study [5] of the validity of the dispersion-relation optical potential for both neutron and proton scattering from ^{208}Pb in an energy interval from -17 to $+40$ MeV, L dependence was again found desirable. An analysis of n-^{40}Ar total cross sections and single-particle binding energies [6] found evidence for a parity-dependent optical potential. The physical origin of the L dependence in the above studies is either attributed [2,4,7,8] to the coupling to inelastic excitations, or to the inadequacy of using Woods-Saxon-shaped optical potentials [2,9], but not to the exchange nonlocality. On the other hand, the optical potential for nucleon-^{4}He scattering, obtained [10] by inversion of theoretical phase shifts calculated by the resonating-group method (RGM) [11], was found to be parity dependent, whether coupling to rearrangement channels was included or not. Coupling to rearrangement channels does make a substantial contribution to nucleon-nucleus scattering [12], and it is possible that this effect may lead to additional L dependences [13].

Although an L dependence of the total optical potential is expected on general theoretical grounds [14,15], it is very difficult to make a clear prediction of what that L dependence should be for practical applications. The purpose of the present study is to investigate what L dependence one should expect in the optical model due to exchange effects alone. We consider only the "knockon" exchange terms, which are included in the Hartree-Fock potential. For nuclei as heavy as ^{16}O, the core exchange terms can be ignored [16]. We first examine the behavior of the direct and exchange microscopic matrix elements of the effective nucleon-nucleon interaction from which the Hartree-Fock potential is obtained. Based on this result we introduce a new local L-dependent optical potential which reflects the properties of the matrix elements, and finally we compare the results of this new optical potential with those of an L-independent local equivalent potential obtained by inversion [17] of the Hartree-Fock scattering phase shifts for the case of n-^{16}O scattering at 20 and 50 MeV [1]. Our new potential differs from another type of L-dependent potential which is based on the Wronskian [18,19] technique. Indeed we find that the L dependence of our potential is much milder and of a different nature than that of Ref. [19].

Our method is based on the observation that, for low values of the incident nucleon's angular momentum L, a local folding potential can be found [20], called $V_H^{(e)}$,

which, as will be explained below, is near to being phase equivalent to the complete Hartree-Fock potential. For large values of L, the exchange effects become negligible, and the conventional Hartree part V_H of the potential suffices. Our overall L-dependent local potential $V_L(r)$ is obtained as a linear superposition of both these potentials:

$$V_L(r) = N_L V_H(r) + N_L^{(e)} V_H^{(e)}(r) \ . \tag{1.1}$$

The phenomenological coefficients N, which are L dependent but r independent, are determined such that (1) the phase shifts obtained from V_L are the same as those of the exact Hartree-Fock potential, and (2) the "error" in the wave function is as small as possible, i.e., it minimizes the mean difference between the wave functions of the nonlocal exact potential, and that obtained from our local L-dependent potential for each value of L. This requirement has apparently not been introduced previously. It eliminates *ab initio* all those families of potentials in which the wave function has a different number of nodes than the nonlocal wave function.

The implementation of these two conditions is described in Sec. III, after a definition of the potential $V_L^{(e)}$ has been given in Sec. II. The justification for this potential is based on the properties of the matrix elements of the complete nonlocal potential evaluated over the scattering wave function. These matrix elements occur because in our treatment of the solution of the nonlocal Schrödinger equation, the scattering wave function is obtained as an expansion on a set of Sturmian basis functions, a procedure which naturally leads to the matrix elements mentioned above. In Sec. III, the potential V_L will be obtained numerically for the case of n-^{16}O scattering, using the same procedures for calculating V_H and $V_H^{(e)}$ from a microscopic N-N interaction as described in a previous study [1]. In Sec. IV, the various partial wave functions will be compared, and finally, in Sec. V, we give a discussion plus a summary.

We also compare the resulting potential V_L with Mackintosh's inversion potential [1]. The fact that the wave functions resulting from our V_L approximate the exact nonlocal wave functions as nearly as well as the wave function based on the inversion potential is a useful result of the present study, because it shows that it is difficult to improve upon the inversion potential, which is L independent and simpler than our V_L.

II. MICROSCOPIC MATRIX ELEMENTS AND THE JUSTIFICATION FOR $V_H^{(e)}$

In this section we show that the matrix elements of $V_H^{(e)}$, taken between the scattering wave functions, are close to the matrix elements of the nonlocal Hartree-Fock potential, for low values of the scattering angular momentum numbers L. The examination of the properties of such matrix elements is what leads to the definition of $V_H^{(e)}$.

The exchange effects give rise to a nonlocal nucleon-nucleus interaction, which, in turn, produces L-dependent effects. This can be seen by examining the Hartree-Fock potential [15]. The local, or Hartree, part is given by

$$V_H(r_0) = \sum_a \int \varphi_a(\vec{r}_1)^* v_{\rm dir}(|\ \vec{r}_1 - \vec{r}_0\ |)\varphi_a(\vec{r}_1) d^3 r_1 \tag{2.1a}$$

and the exchange part for the knockon process is given by the integral kernel

$$K(\vec{r}_0, \vec{r}_0') = -\sum_a \varphi_a(\vec{r}_0)^* v_{\rm exch}(|\ \vec{r}_0 - \vec{r}_0'\ |)\varphi_a(\vec{r}_0') \ . \tag{2.1b}$$

The fact that the microscopic N-N effective interactions $v_{\rm dir}$ and $v_{\rm exch}$ are also density dependent is not only explicitly indicated in the above, but is taken into account in what follows. The procedure for doing so is described in Refs. [1,20]. Only the central part of the N-N interaction is included here, i.e., spin-orbit and tensor effects are left out. The single-particle bound-state wave functions are denoted by φ_a, where a represents the bound-state quantum numbers. The exchange kernel is not L dependent, but its projection onto the angular-momentum space, $K_L(r_0, r_0')$ becomes L dependent. This can be seen as follows. When the Schrödinger equation is solved by first decomposing the scattering wave function $\Psi(\vec{r}_0)$ into partial waves,

$$\Psi(\vec{r}_0) = \sum_{L,M} \psi_{LM}(\vec{r}_0) \tag{2.2a}$$

with

$$\psi_{LM}(\vec{r}_0) = \frac{1}{r_0} R_L(r_0) Y_{LM}(\hat{r}_0) \ , \tag{2.2b}$$

then integration over the Y_{LM}'s results in the definition of the projected kernel [1,20]

$$K_L(r_0, r_0') = \int\int Y_{LM}^*(\hat{r}_0) K(\vec{r}_0, \vec{r}_0') Y_{LM}(\hat{r}_0') r_0 r_0' d\Omega_0 d\Omega_0' \ . \tag{2.3}$$

Even though $K(\vec{r}_0, \vec{r}_0')$ is rotationally invariant, K_L is nevertheless L dependent since it depends on the direction between $\vec{r}_0$ and $\vec{r}_0'$. As an illustration, K_L for n-^{16}O scattering is shown in Figs. 1 and 2 for an incident energy of 20 MeV. The L dependence is illustrated more clearly in Fig. 2, which shows the diagonal value of the real part of K_L, i.e., the result when $r_0 = r_0'$, as a function of r_0 for various values of L. The effective microscopic, density-dependent, interaction is taken from Ref. [21] and

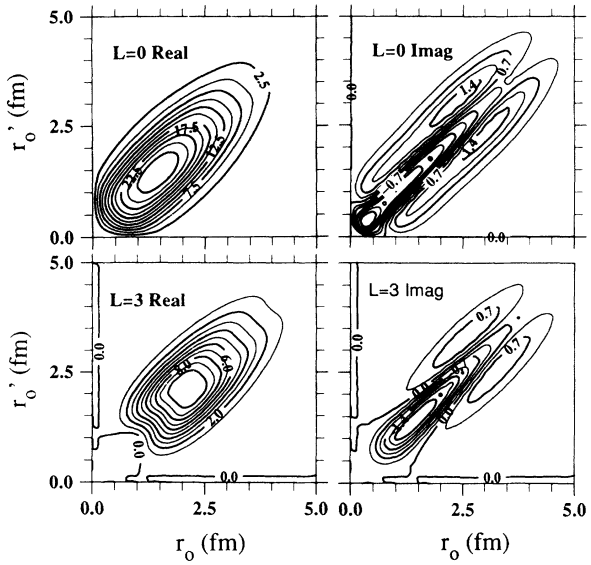

FIG. 1. Real part of the exchange kernel $K_L(r_0, r_0')$ for n-^{16}O scattering at an incident energy of 20 MeV (lab). This kernel has been defined in Eq. (2.3).

the bound nucleon states are obtained in a harmonic-oscillator well in the absence of a spin-orbit interaction, as is explained in detail in Ref. [1].

There are several methods for solving the nonlocal Schrödinger equation [19,22–24]. Our method consists

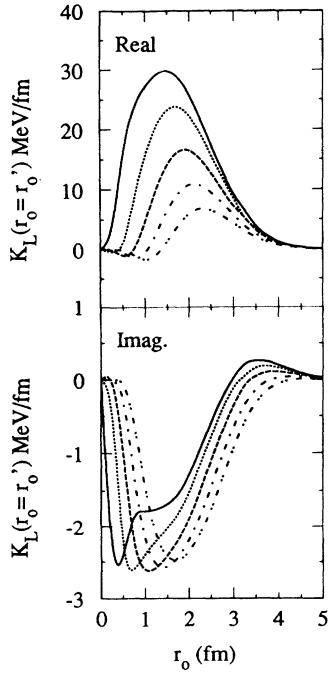

FIG. 2. Diagonal part ($r_0 = r_0'$) of the exchange kernel displayed in Fig. 1. The upper and lower panels show the real and imaginary parts, respectively. The solid, dotted, dashed, dash-dotted, and dash-double-dotted curves correspond to values of the angular-momentum number L of 0, 1, 2, 3, and 4, respectively.

in expanding each partial wave into a superposition of basis states $\psi^{(j)}$:

$$\psi_{LM}(\vec{r}_0) = \psi^{(0)}_{LM}(\vec{r}_0) + \sum_j c^{(j)}_{LM}\psi^{(j)}_{LM}(\vec{r}_0) \ , \tag{2.4}$$

where $\psi^{(0)}_{LM}$ represents the incident plane wave part of the scattering wave, i.e., it is of the form

$$\psi^{(0)}_{LM} = j_L(kr_0)Y_{LM}(\hat{r}_0) \ , \tag{2.5a}$$

with k the wave number of the incident wave, and the $\psi^{(j)}_{LM}$'s are the Sturmian basis functions of the form

$$\psi^{(j)}_{LM} = j_L(K_j r_0)Y_{LM}(\hat{r}_0) \ , \tag{2.5b}$$

where the K_j's are complex Sturmian wave numbers determined by the boundary conditions, as is described in Ref. [25]. With the expansion (2.4), the solution of the Schrödinger equation leads [25] to matrix equations for the coefficients $C^{(j)}$, which involve matrices whose matrix elements, when generalized to the Hartree-Fock potential case are of the type [20]

$$M^{(a)}_{jj'} = \langle \varphi_a(\vec{r}_1)\psi^{(j)}(\vec{r}_2)v_{\rm dir}\varphi_a(\vec{r}_1)\psi^{(j')}(\vec{r}_2)\rangle - \langle \varphi_a(\vec{r}_1)\psi^{(j)}_{LM}(\vec{r}_2)v_{\rm exch}\psi^{(j')}_{LM}(\vec{r}_1)\varphi_a(\vec{r}_2)\rangle \ . \tag{2.6}$$

The brackets $\langle\,\rangle$ denote integration over d^3r_1 and d^3r_2 together with complex conjugation of the bra functions (with the exception that the Sturmian wave numbers K_j are left unaltered).

The steps which lead to the definition of $V^{(e)}_H$ will now be described. The subscripts L and M are suppressed in the discussion which follows. Since the microscopic direct and exchange interactions are *not* equal, it is convenient to rewrite Eq. (2.6) in the form

$$M^{(a)}_{jj'} = \langle \varphi_a\psi^{(j)}(v_{\rm dir} - v_{\rm exch})\varphi_a\psi^{(j')}\rangle + \langle \varphi_a\psi^{(j)}v_{\rm exch}(\varphi_a\psi^{(j')} - \psi^{(j')}\varphi_a)\rangle \ . \tag{2.7}$$

The terms in the second line above contain only angular momentum components of relative motion between particles 1 and 2 which are odd. This can be seen by rewriting Eq. (2.7) in the coordinates of relative motion between particles 1 and 2, i.e., if one changes to the variables $\vec{r} = \vec{r}_1 - \vec{r}_2$ and $\vec{R} = (\vec{r}_1 + \vec{r}_2)/2$, and if one decomposes the product of the two wave functions into even (E) and odd (O) components under the change of $\vec{r}$ into $-\vec{r}$:

$$\varphi_a(\vec{r}_1)\psi^{(j)}(\vec{r}_2) = E_{aj}(\vec{r},\vec{R}) + O_{aj}(\vec{r},\vec{R}) \ , \tag{2.8a}$$

$$\psi^{(j)}(\vec{r}_1)\varphi_a(\vec{r}_2) = E_{aj}(\vec{r},\vec{R}) - O_{aj}(\vec{r},\vec{R}) \ . \tag{2.8b}$$

The second equation follows from the fact that if $\vec{r}_1$ is interchanged with $\vec{r}_2$, then $\vec{r} \to -\vec{r}$. With that notation, the second line of Eq. (2.7) can be written in

the form $2\langle O_{aj} v_{\rm exch} O_{aj'}\rangle$, if one remembers that the matrix element between an even and an odd state vanishes, $\langle EvO\rangle = 0$, since v is an even function of $\vec{r}$. Finally defining the microscopic interaction

$$v_e = v_{\rm dir} - v_{\rm exch} \ , \tag{2.9}$$

we can rewrite Eq. (2.7) in the form

$$M^{(a)}_{jj'} = \langle \varphi_a \psi^{(j)} v_e \varphi_a \psi^{(j')}\rangle + 2\langle O_{aj} v_{\rm exch} O_{aj'}\rangle \ . \tag{2.10}$$

A careful study was made [20] of the size of the odd component O in the product wave function $\varphi_a\varphi_b$ of two nucleons, where φ_b approximates the single-particle scattering wave function $\psi^{(j)}_{LM}$. The result was found to depend on the angular-momentum value L (relative to the center of the nucleus) of the scattered wave φ_b. For small values of L, the O part was found to be considerable less than the E part. This is illustrated in Table II in the Appendix, which lists the contribution to M_{jj}, from the various components of relative angular momentum l contained in the wave function $\varphi_a\varphi_b$. A result of this type is illustrated in Fig. 3. However, in this case the scattering wave function is represented by a Sturmian function

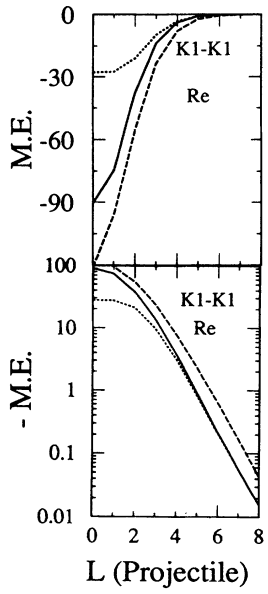

FIG. 3. Matrix element $M_{jj'}$ for n-^{16}O scattering as a function of the projectile's angular-momentum L. The lower panel, apart from the sign, represents the same matrix element (ME) on a logarithmic scale. The solid lines illustrate the complete matrix element (direct−exchange) as defined in Eqs. (2.6) and (2.11). The dotted lines illustrate only the direct part of this ME. The dashed lines represent the direct ME of the component v_e of the nucleon-nucleon interaction, defined in Eq. (2.9). The wave function ψ_j of the nucleon in the continuum is given by the Sturmian function defined in Eq. (2.5b), and $K_j = K_{j'}$ has the value $0.97 - 0.10i$ fm^{-1}, which is at the center of the important range. The bound nucleons are represented by harmonic-oscillator functions, as described in the text. Only the real parts of these matrix elements are shown. The units are in MeV fm^3.

$\psi^{(j)}_{LM}$ as given by Eq. (2.5), and the value of the matrix elements are calculated in the laboratory frame from Eq. (2.7) by using the analytical expressions developed in Ref. [20]. Furthermore, the matrix elements are summed over the occupied single-particle states in ^{16}O,

$$M_{jj'} = \sum_a M^{(a)}_{jj'} \ . \tag{2.11}$$

In Fig. 3, the Sturmian momenta K_j and $K_{j'}$ are both equal to the value $(0.908-0.096i)$ fm^{-1}, which is near the center of the range of discrete values which are needed in the expansion (2.4) of the scattering wave for an incident energy of 20 MeV. The dashed line represents the first term in Eq. (2.10), the solid line is the complete result for $M_{jj'}$ given by Eq. (2.6), and the dotted line is the direct part of $M_{jj'}$ given by the first line of Eq. (2.6). The difference between the dotted and solid lines represents the contribution from the exchange term [second line of Eq. (2.6)] and the difference between the dashed and the solid lines is the contributions from the term given by the second line of Eq. (2.7). The dashed line lies considerably closer to the solid line than the dotted line, which shows that the first term in Eq. (2.10) provides a better approximation to the matrix element than the direct term alone, for low partial waves. Beyond $L = 4$, the reverse is seen to be the case. The logarithmic scale in the lower panel of Fig. 3 illustrates this large L behavior more clearly. When the two Sturmian functions are not the same, i.e., when $K_j \neq K_j$, the agreement between the dashed and solid lines becomes less good, as is shown in Fig. 4, but the values of these nondiagonal matrix elements are not as large as the diagonal ones. Thus for the low partial waves, the local potential

$$V^{(e)}_H(r_0) = \sum_a \int \varphi_a(\vec{r}_1) v_e(|\,\vec{r}_1 - \vec{r}_0\,|)\varphi_a(\vec{r}_1) d^3 r_1 \ , \tag{2.12}$$

which arises from the first line of Eq. (2.7) and which is obtained by folding the even part of the microscopic nucleon-nucleon effective interaction over the nucleon wave functions of the target nucleus, gives a better approximation to the nonlocal Hartree-Fock potential than

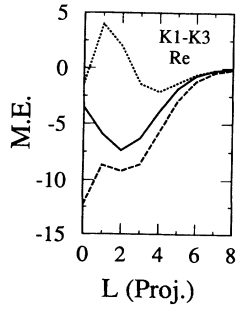

FIG. 4. Similar to the top panel of Fig. 3. However, the two Sturmian functions have different wave numbers, K_1 is as in Fig. 3, and $K_3 = 1.99 - 0.03i$ fm^{-1}.

the Hartree part, based on $v_{\rm dir}$. The subscript "e" of the microscopic potential defined in Eq. (2.9) stands for "even." This is because if one expresses $v_{\rm dir}$ and $v_{\rm exch}$ in terms of the pieces which act on the even and odd, singlet and triplet components of the interacting pair of nucleons, averaged over spin and isospin degrees of freedom of these nucleons,

$$v_{\rm dir} = (9v^{TO} + 3v^{SE} + 3v^{TE} + v^{SO})/4 \ , \qquad (2.13a)$$

$$v_{\rm exch} = (9v^{TO} - 3v^{SE} - 3v^{TE} + v^{SO})/4 \ , \qquad (2.13b)$$

one obtains for v_e the result

$$v_e = (3v^{SE} + 3v^{TE})/2 \ , \qquad (2.14)$$

i.e., v_e contains only the contribution from the even states of the relative nucleon-nucleon motion. If an "odd" interaction is similarly defined as $v_o = v_{\rm dir} + v_{\rm exch}$, then one obtains

$$v_o = (9v^{TO} + v^{SO})/2 \ . \qquad (2.15)$$

In this notation, the complete matrix element defined in Eq. (2.6) is given by

$$M^{(a)}_{jj'} = \langle E v_e E \rangle + \langle O v_o O \rangle \ , \qquad (2.16)$$

which shows that the exchange effect automatically sorts out the even (odd) pieces of the wave function with the even (odd) pieces of the nucleon-nucleon interaction, as is to be expected.

III. THE L-DEPENDENT LOCAL POTENTIAL

In Sec. II, the matrix elements of the Hartree-Fock potential were decomposed into the direct matrix elements of the even part of the N-N interaction, plus a remainder which comes from a nonlocal piece of the interaction, as is described by Eq. (2.7). For small values of L, the former part provided the major contribution to the total matrix element and gave rise to the local potential $V^{(e)}_H$, and the latter could be considered as a small L-dependent correction. For large values of L the exchange contribution becomes small, and the conventional Hartree part V_H of the potential gives the major contribution. It is thus natural to define the L-dependent potential V_L as a linear combination between these two:

$$V_L(r) = N_L V_H(r) + N^{(e)}_L V^{(e)}_H(r) \ ,$$

as was already described in the Introduction in Eq. (1.1). The numerical implementation of the above procedure will now be described for the case of n-^{16}O scattering.

The Hartree potentials V_H and $V^{(e)}_H$, defined in Eqs. (2.1a) and (2.12), respectively, are calculated analytically using the same methods developed [20] for calculating the matrix elements $M_{jj'}$ defined in Eq. (2.6). The analytic evaluation is possible because the functions involved in the integrals are simple: The effective density dependent, complex, N-N interaction [21] is given by a sum of Gaussian functions, and the harmonic oscillator bound-state single-particle wave functions are given in terms of powers of r times Gaussian functions. Details and the values of all parameters are given in Ref. [1]. The two Hartree potentials V_H and $V^{(e)}_H$ are illustrated in Figs. 5 and 6, for the two energies 20 and 50 MeV, respectively. The inversion potentials obtained from the scattering matrix elements S_L in Ref. [1] are also shown for comparison. As is illustrated in the figures, the inversion potential is bracketed between the two Hartree potentials for the real part, but not for the imaginary part.

The four parameters contained in the two complex phenomenological coefficients N_L and $N^{(e)}_L$ are determined by a numerical Newton-Cotes procedure so as to satisfy two requirements: (1) The scattering matrix elements S_L obtained rigorously from the microscopic nonlocal (nl) Hartree-Fock potential and those obtained from the local (l) potential V_L should agree for each value of L; and (2) the radial partial wave function $R^{(l)}_L$ based on V_L, should approach the one obtained from the nonlocal Hartree-Fock potential, $R^{(\rm nl)}_L$, in the mean, i.e., the deviation

$$E_L = \int_0^\infty | \, R^{(\rm nl)}_L(r) - R^{(l)}_L(r) \, |^2 \, dr \qquad (3.1)$$

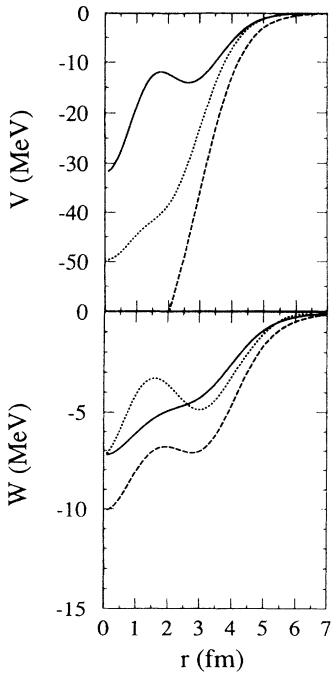

FIG. 5. Comparison between two Hartree potentials V_H, $V^{(e)}_H$, and an inversion potential for n-^{16}O scattering at 20 MeV. The solid and dashed lines represent the Hartree potentials, defined in Eqs. (2.1a) and (2.12), obtained, respectively, with the full direct part of the N-N interaction and the even part only of this interaction. The dotted line represents the potential obtained by "inversion" [1] of the scattering phase shifts. The upper (lower) panel represents the real (imaginary) part of these potentials.

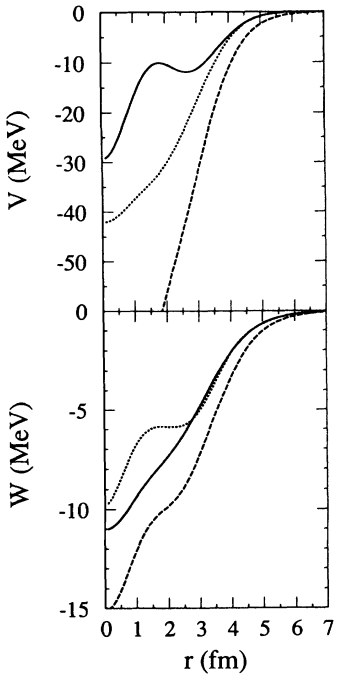

FIG. 6. Same as Fig. 5 for a neutron incident energy of 50 MeV.

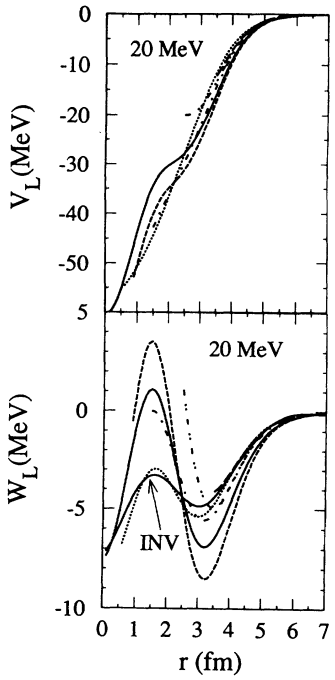

FIG. 7. Angular-momentum-dependent potential for n-^{16}O scattering at 20 MeV. This potential is defined by Eq. (1.1). The real and imaginary parts are represented in the upper and lower panels, respectively. The solid, dotted, dashed, dash-dotted, dash-double-dotted, and long-dashed lines represent the potentials for the angular-momentum L of 0, 1, 2, 3, 4, and 5, respectively. For each value of L the potentials are shown only in the radial region where the absolute value of the corresponding wave function is larger than 0.1. The inversion potential is shown also for the imaginary part.

should be a minimum. This condition ensures that the number of nodes in the local equivalent wave function be the same as that of the rigorous nonlocal wave function. The numerical values obtained in our searches turned out to be unique.

The results for the N_L's are listed in Table I, and the corresponding L-dependent potentials are plotted in Figs. 7 and 8. In these figures the values of the potentials are suppressed in the radial interval where the corresponding radial wave functions have a magnitude less than 0.1, so as to emphasize only the region where the potential has a significant effect. The normalization of the wave functions is such that asymptotically they are of the form $\exp(i\delta_L)\sin(kr - L\pi/2 + \delta_L)$, where δ_L is the complex phase shift. One sees from these figures that the real part of V_L is not strongly L dependent, in contrast to what is the case when the potential is determined by means of the Wronskian method [19]. Also of interest is the result that the L dependence for the imaginary part

TABLE I. Coefficients N_L for the determination of the angular-momentum-dependent potential $V_L(r)$, according to Eq. (1.1).

	20 MeV				50 MeV				50 MeV[a]	
	N_L		$N_L^{(e)}$		N_L		$N_L^{(e)}$		N_L	
L	Re	Im	Re	Im	Re	Im	Re	Im	Re	Im
0	0.842	0.674	0.357	−0.233	0.305	0.669	0.464	−0.186	0.826	0.112
1	−0.425	0.298	0.712	−0.049	−0.113	0.362	0.564	−0.064	0.805	0.092
2	0.785	1.022	0.463	−0.335	−0.321	0.451	0.642	−0.066	0.801	0.087
3	0.116	0.460	0.596	−0.149	0.916	0.551	0.318	−0.208	0.790	0.088
4	1.190	1.056	0.104	−0.451	0.571	0.225	0.347	−0.083	0.771	0.005
5	1.305	0.424	−0.022	−0.200	0.201	0.548	0.464	−0.191	0.712	−0.042
6	1.137	0.223	0.009	−0.105	1.358	0.268	−0.071	−0.151	0.626	0.022
7	1.061	0.135	0.016	−0.062	1.164	0.077	−0.025	−0.058	0.508	0.164
8					1.078	0.031	−0.007	−0.031	0.350	0.329
9					1.042	0.013	−0.003	−0.018	0.170	0.475
10					1.025	0.005	−0.003	−0.012	−0.001	0.579

[a]For this case V_H in Eq. (1.1) is replaced by the 20 MeV Woods-Saxon potential of Petler *et al.* [26], and $V_H^{(e)}$ is replaced by zero.

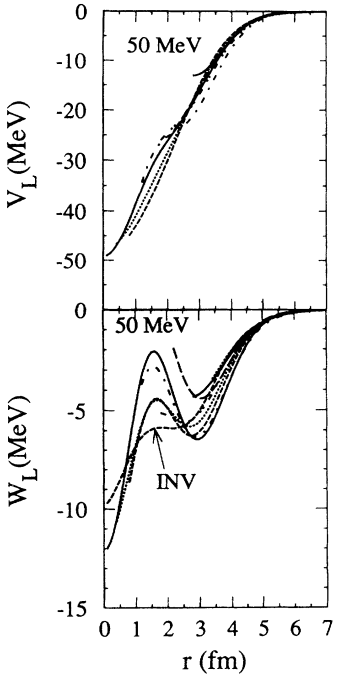

FIG. 8. Same as Fig. 7 for a neutron energy of 50 MeV.

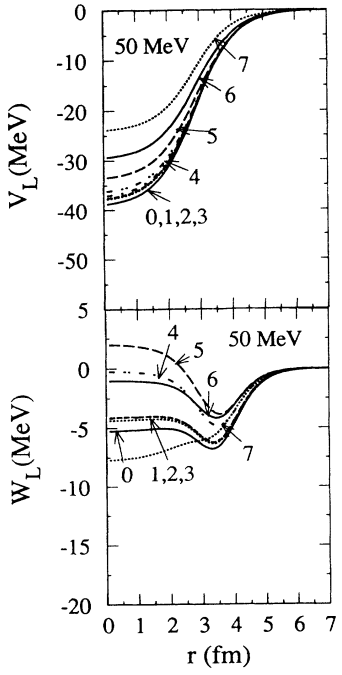

FIG. 9. An L-dependent Woods-Saxon potential at 50 MeV which gives the same phase shifts as the exact Hartree-Fock potential. It is the product of a complex factor N_L times the Woods-Saxon potential of Ref. [26] which fits n-^{16}O scattering at 20 MeV. The numbers near the arrows indicate the value of the angular-momentum L. The tips of the arrows are located at the points where the absolute value of the wave functions is larger than 0.1, i.e., only the portion of the curves to the right of the tip of the arrow are of importance.

is more pronounced at the lower energy (20 MeV) than at the higher one (50 MeV), and that the nature of their ondulatory shape is similar to that of the inversion potential. The average over L of the real part of the V_L's is not in good agreement with the real part of the inversion potential. For $E = 50$ MeV, the latter is shallower than V_L by about 8 MeV near the origin, and deeper by about 5 MeV near 3 fm. At 20 MeV this difference is of the same nature and a little more pronounced.

At 20 MeV the inversion potential was found [1] to be quite close to the phenomenological Woods-Saxon optical potential of Petler *et al.* [26], especially its real part. One can obtain a measure of how the shape of the potential changes with energy, if one uses the same Woods-Saxon potential of Ref. [26] at 50 MeV, but multiplied by a factor N_L determined such that the resulting phase shifts agree with the microscopic results for the Hartree-Fock potential. If N_L changes weakly with L, then the shape of the 20 MeV Woods-Saxon potential would also be suitable at 50 MeV. The result is shown in Fig. 9. One sees that the imaginary part of the potential changes quite significantly with L, and the real part of the potential changes visibly once L is larger than 4. This shows that if the data are fit with a Woods-Saxon potential, then the microscopic calculation suggests that the shape of this potential should change with energy. It is premature to investigate whether the changes found here are compatible with experimental studies [9], because the dynamic polarization effects are left out of the present investigation.

IV. COMPARISON BETWEEN LOCAL AND NONLOCAL WAVE FUNCTIONS

It is well known [27] that if two wave functions have the same asymptotic behavior (i.e., they are phase equivalent) and also have the same number of nodes in the interior of the nuclear region, but if one wave function is the solution of a nonlocal potential, while the other is the solution of a local equivalent potential (LEP), then the two wave functions will differ in the nuclear interior. The ratio of two such wave functions is the Perey damping factor, which is an important ingredient in distorted-wave Born approximation calculations. Since our L-dependent potential is determined by the requirement that the local and nonlocal wave functions be as close to each other as possible, an illustration of these wave functions is of interest.

The comparison between two local equivalent wave functions and the exact nonlocal wave function is illustrated in Figs. 10–12, for various values of L, for n-^{16}O scattering at an incident energy of 50 MeV. The exact nonlocal wave function is shown by means of the solid lines, the functions generated by V_L, and the inversion potential are shown by dotted and dashed lines, respectively. The general trend of the real part of the wave functions is shown in Fig. 10. An enlarged view of the real and imaginary parts is given in Figs. 11 and 12, respectively. The amplitude of the imaginary parts is larger than that for the real parts (note the suppressed

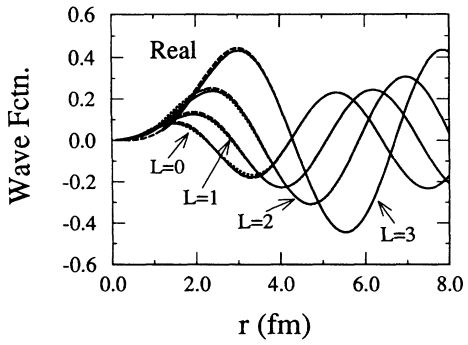

FIG. 10. Real part of the scattering wave functions for various values of the angular-momentum L. The solid curves illustrate the wave functions based on the exact Hartree-Fock potential, the dotted curves represent the results for the L-dependent potentials V_L, and the dotted curves are for the L-independent inversion potential. The normalization of these wave functions is described in the text.

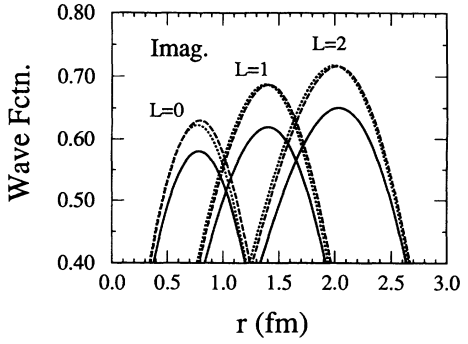

FIG. 12. Same as Fig. 11 for the imaginary part of the wave functions.

scale in Fig. 12), but the percent deviation between the amplitudes of the local and nonlocal wave functions is approximately the same, of the order 10–15 % for small values of the radial distance r. It is interesting that the two local wave functions nearly coincide with each other, which is especially the case for the imaginary parts. For the real parts, the function obtained with V_L gives only a slightly better approximation to the exact nonlocal wave function than does the local function based on the inversion potential. This shows that the inversion potential not only produces the correct phase shifts for all values of L, but it also reproduces the nonlocal wave functions nearly optimally.

V. SUMMARY AND CONCLUSIONS

A new local Hartree potential $V_H^{(e)}$ was defined, such that for low angular-momentum values L of the scattered wave the matrix elements of $V_H^{(e)}$ taken between scattering wave functions provide a better approximation to the matrix elements of the exact Hartree-Fock potential than do the matrix elements of the conventional Hartree potential V_H. This result is based on two observations [20]:

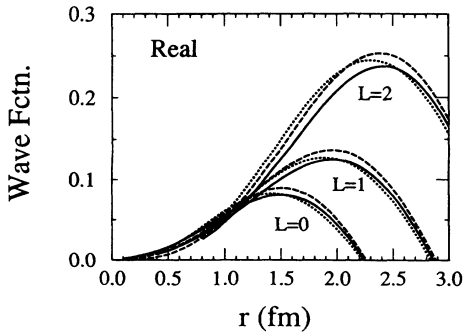

FIG. 11. Same as Fig. 10 in an enlarged scale.

(1) The product of two single-particle wave functions, the one bound, the other in the continuum, has components of relative motion which are predominantly of even parity. This can be seen by expanding the product of two such wave functions as a superposition of states of relative angular momenta l'. One finds that the component with largest amplitude occurs for $l' = 0$. However, the components with $l' \neq 0$ increase relative to the $l' = 0$ component as the angular momentum (relative to the nucleus) of the continuum nucleon increases compared to the angular momentum of the bound nucleon. (2) The matrix elements described above can be reorganized into two parts, one which is the direct matrix element of a certain piece, v_e, of the microscopic N-N interaction and a second part which contains only the odd components of the relative motion of the two interacting nucleons. In view of observation (1) the second part of the matrix element is small compared to the first part and hence the Hartree potential based on v_e, namely, $V_H^{(e)}$, plays a major role in the determination of the optical potential for nucleon-nucleus scattering for the low partial waves. For large values of L the exchange terms become relatively unimportant and the conventional Hartree potential gives the major contribution to the optical potential.

Based on the above insights, an L-dependent local optical potential is defined as a linear combination of the two Hartree potentials mentioned previously. The coefficients $N_L^{(e)}$ and N_L are independent of the radial distance r but depend on L, so as to express the fact that the relative importance of $V_H^{(e)}$ and V_H depends on L. These two coefficients are complex and therefore represent four parameters. These are determined numerically by a Newton-Cotes procedure from the requirements that (1) the scattering phase shifts obtained from V_L be numerically the same as those for the exact nonlocal Hartree-Fock potential, and (2) the local and nonlocal partial wave functions be as close to each other in the mean as possible. It should be kept in mind that the present study leaves out the L dependence which is expected to occur due to rearrangement processes [28] or to dynamic polarization effects [7,8,29].

A numerical example for the potentials V_L is given for n-^{16}O scattering at two energies. The Hartree-Fock potential is obtained by folding the density-dependent ef-

fective nucleon-nucleon interaction given by Yamaguchi, Nagata, and Matsuda [21] over the harmonic-oscillator wave functions of the target nucleons, similarly to what was done in a previous study of the equivalent inversion potential [1]. The real part of V_L turns out to depend on L very mildly, in contrast to what was found [19] to be the case for a different L-dependent potential based on a Wronskian method [18]. The imaginary part of V_L is more L dependent than the real part, and the L dependence is more pronounced at the lower energy. The radial wave functions of the exact nonlocal potential were compared with those of V_L, and also with those of a second local equivalent, but L-independent, potential obtained from the scattering phase shifts by an inversion method [1]. The two local wave functions differ from the nonlocal wave function in approximately the same manner. Neither V_L nor the inversion potential is of a Woods-Saxon shape. If a Woods-Saxon shape is nevertheless used to fit the data, then our Fig. 9 shows that, in order to simulate the exchange process, an L dependence may well be expected. Our study thus provides some basis for the use of L-dependent imaginary potentials, found necessary in a study of n-Pb scattering at low energies [2–5].

In summary, we have introduced a new L-dependent local potential which is phase equivalent to a microscopic nonlocal Hartree-Fock potential, and which minimizes the difference between the corresponding (local and nonlocal) scattering radial wave functions. This potential is compared with an L-independent potential determined previously [1] by an inversion method for the case of n-^{16}O scattering. The comparison between these two potentials shows that L dependence is not required in order to simulate the exchange nonlocality and still obtain good scattering wave functions, provided that the radial shape of the L-independent potential is carefully chosen.

ACKNOWLEDGMENTS

One of us (D.L.) is grateful for financial support received from the University of Connecticut Research Foundation. Also the computational support from the University of Connecticut Computer Center and from the computing facilities of the Physics Department are much appreciated.

APPENDIX: CONTRIBUTION FROM RELATIVE ANGULAR-MOMENTUM COMPONENTS TO THE MATRIX ELEMENTS

The solution of the nonlocal Hartree-Fock Schrödinger equation by the method of expansion of the scattering wave into a basis set of functions $\psi^{(j)}_{LM}$ according to Eq. (2.4), requires the calculation of the matrix elements $M_{jj'}$ given by Eq. (2.6). The functions φ_a represent the single-particle bound states, which are given by the expression

$$\varphi_a(\vec{r}_1) = N_a r_1^{L_1} \exp(-b_a r_1^2) Y_{L_1 M_1}(\hat{r}_1) \ , \qquad \text{(A1)}$$

while the functions $\psi^{(j)}_{LM}$ are given by Eq. (2.5b). For the calculations [20] reported in this appendix, $\psi^{(j)}_{LM}$ will be approximated by a Gaussian function of the type given by Eq. (A1),

$$\psi^{(j)}_{LM} \to \varphi_b(\vec{r}_2) = N_b r_2^{L_2} \exp(-b_b r_2^2) Y_{L_2 M_2}(\hat{r}_2) \ , \qquad \text{(A2)}$$

where the Gaussian parameter b_b has a different value from the one for the bound-state wave function, b_a. The quantities L_1 and L_2 represent the angular-momentum numbers of each particle relative to the center of the nucleus, and the normalization factors N are determined such that the integral over all space of the absolute value squared of each wave function is unity.

With the Gaussian choice for both wave functions φ_a and φ_b given by Eqs. (A1) and (A2), it is possible to carry out analytically the decomposition of the product of the two wave functions into states of relative angular momentum l in the space of the coordinates $\vec{r} = \vec{r}_1 - \vec{r}_2$ and $\vec{R} = (\vec{r}_1 + \vec{r}_2)/2$,

$$\varphi_a(\vec{r}_1)\varphi_b(\vec{r}_2) = \sum_{lm} \chi_{lm}(\vec{R}, r) Y_{lm}(\hat{r}) \ . \qquad \text{(A3)}$$

The quantities χ depend on the values of L_1 and L_2, as well as on the Gaussian parameters b_a and b_b. This decomposition requires a great deal of angular-momentum algebra plus the use of Moshinsky brackets [20]. In terms of this expansion the matrix elements (2.6) described in Chap. 2 of Ref. [20] can be obtained as a sum over the contributions from the various relative angular-momentum components l. The analytical expressions are given in Chap. 2 of Ref. [20]. A computer code was written and the total result for the matrix element, calculated in terms of the relative angular-momentum contributions, was compared numerically with the calculation done in the "laboratory" coordinate space $\vec{r}_1$ and $\vec{r}_2$. Agreement to four significant figures was obtained. In the numerical results given in the tables below, the angular momentum L_1 (relative to the nucleus) of the "bound" particle is set to zero, the value of L_2 for the "scattered"

TABLE II. Contribution of various relative angular-momentum components to the matrix elements ϕ_{ab} defined in Eq. (A4). The units are in MeV. The single-particle states are represented by harmonic-oscillator wave functions, Eqs. (A1) and (A2). The N-N potential is a Gaussian function of the relative distance between the two interacting particles. The angular-momentum L_1 of the particle in state a is set equal to zero, that in stable b is L_2, and l is one of a set of the relative angular momenta between the two interacting particles, which occur in the expansion of the wave function product given by Eq. (A3). The values of all parameters defining the wave functions and the potential are given in the text.

l	$L_2 = 0$	$L_2 = 1$	$L_2 = 4$
0	−2.7614	−1.8774	−0.5929
1	−0.0556	−0.2279	−0.2511
2	−0.0006	−0.0047	−0.0388
3			−0.0031
Total	−2.8177	−2.1100	−0.8861

TABLE III. Contribution of various relative angular-momentum components to the real part of the matrix elements M_{ab} defined in Eq. (A5). Direct and exchange terms are both present. The units are in MeV. The microscopic N-N potential is a superposition of Gaussian functions given in Ref. [21], which depend on the energy of the incident particle, 20 and 50 MeV. Everything else is the same as in Table II.

	20 MeV			50 MeV		
l	$L_2=0$	$L_2=1$	$L_2=4$	$L_2=0$	$L_2=1$	$L_2=4$
0	−5.3963	−3.7111	−1.2111	−3.8777	−2.6672	−0.8701
1	0.0152	0.0591	0.0326	0.0152	0.0591	0.0326
2	−0.0008	−0.0061	−0.0479	−0.0005	−0.0039	−0.0308
3		0.0002	0.0084		0.0002	0.0084
Total	−5.3825	−3.6578	−1.2183	−3.8630	−2.6118	−0.8599

particle ranges from 0 to 4, and the Gaussian parameters have the values $\beta_a = 0.04$ fm^{-2} and $\beta_b = 0.10$ fm^{-2}.

The results for a matrix element which does not involve exchange

$$\phi_{ab} = \langle \varphi_a(\vec{r}_1)\varphi_b(\vec{r}_2) V_0 e^{-\alpha r^2} \varphi_a(\vec{r}_1)\varphi_b(\vec{r}_2)\rangle \tag{A4}$$

is given in Table II for the following values of the parameters: $V_0 = -66.92$ MeV, $\alpha = 0.415$ fm^{-2}. This table shows that the importance of the contributions from the high values of relative angular-momentum l increases as the angular-momentum L_2 of the "scattered" particle increases.

Table III lists the l contributions to a matrix element which has direct and exchange terms:

$$M_{ab} = \langle \varphi_a(\vec{r}_1)\varphi_b(\vec{r}_2) v_{\rm dir} \varphi_a(\vec{r}_1)\varphi_b(\vec{r}_2)\rangle - \langle \varphi_a(\vec{r}_1)\varphi_b(\vec{r}_2) v_{\rm exch} \varphi_b(\vec{r}_1)\varphi_a(\vec{r}_2)\rangle \ . \tag{A5}$$

The microscopic potentials $v_{\rm dir}$ and $v_{\rm exch}$ are taken from Ref. [21], however, no density dependence is included for the calculations in this appendix. The result is similar to that of Table II, i.e., the importance of the contributions from the high-l values increases with L_2.

In the presence of exchange terms, it useful to decompose the matrix element M_{ab} into two parts, as is discussed in connection to Eq. (2.7),

$$M_{ab} = M'_{ab} + M''_{ab} \ , \tag{A6}$$

where the first term has no exchange contributions,

$$M'_{ab} = \langle \varphi_a(\vec{r}_1)\varphi_b(\vec{r}_2) v_e \varphi_a(\vec{r}_1)\varphi_b(\vec{r}_2)\rangle \ , \tag{A7}$$

$$M''_{ab} = \langle \varphi_a(\vec{r}_1)\varphi_b(\vec{r}_2) v_{\rm exch}[\varphi_a(\vec{r}_1)\varphi_b(\vec{r}_2) - \varphi_b(\vec{r}_1)\varphi_a(\vec{r}_2)]\rangle \ . \tag{A8}$$

In Table IV, the contributions from the various relative angular-momentum components l to both M' and M'' are listed. As expected, the importance of the high values of l increases with L_2 for both M' and M''. As a result, the contribution of M'' to M is small for small values of L_2, which is the basis for the definition of the L-dependent potential V_L in Eq. (1.1). In all the results above the scattering wave function was approximated by a Gaussian, Eq. (A2). That approximation is removed in Sec. II, and the Sturmian functions of Eq. (2.5b) are

TABLE IV. Contribution of various relative angular-momentum components to the real part of the matrix elements M'_{ab} and M''_{ab}, defined in Eqs. (A7) and (A8), respectively. The units are in MeV. The energy of the incident particle is 20 MeV. Everything else is the same as in Table III.

	20 MeV				50 MeV			
	$L_2=0$		$L_2=4$		$L_2=0$		$L_2=4$	
l	M'_{ab}	M''_{ab}	M'_{ab}	M''_{ab}	M'_{ab}	M''_{ab}	M'_{ab}	M''_{ab}
0	−5.3969		−1.2111		−3.8777		−0.8701	
1	−0.0839	0.0991	−0.3896	0.4222	−0.0597	0.0749	−0.2811	0.3137
2	−0.0008		−0.0479		−0.0005		−0.0308	
3			−0.0057	0.0141			−0.0033	0.0118
Total	−5.4817	0.0991	−1.6548	0.4364	−3.9379	0.0749	−1.1853	0.3255

used instead. The values of M' and M'' are given, respectively, by the first and second lines in Eq. (2.7), whose evaluation does not require the decomposition into relative angular-momentum states. The numerical results displayed in Figs. 3 and 4 show that M' is a better approximation to M than the term given by the first line of Eq. (2.6), for small values of the angular momentum of the projectile.

[1] G. H. Rawitscher, D. Lukaszek, R. S. Mackintosh, and S. G. Cooper, Phys. Rev. C **49**, 1621 (1994).

[2] D. J. Horen, C. H. Johnson, and A. D. MacKellar, Phys. Lett. **161B**, 217 (1985); D. J. Horen, C. H. Johnson, J. F. Fowler, A. D. MacKellar, and B. Castel, Phys. Rev. C **34**, 429 (1986); C. H. Johnson and R. R. Winters, *ibid.* **37**, 2340 (1988).

[3] C. H. Johnson, D. J. Horen, and C. Mahaux, Phys. Rev. C **36**, 225 (1987).

[4] J. P. Jeukenne, C. H. Johnson, and C. Mahaux, Phys. Rev. C **38**, 2573 (1988).

[5] M. L. Roberts, P. D. Felsher, G. J. Weisel, Z. Chen, C. R. Howell, W. Tornow, R. L. Walter, and D. J. Horen, Phys. Rev. C **44**, 2006 (1991).

[6] C. H. Johnson, R. F. Carlton, and R. R. Winters, Phys. Rev. C **44**, 657 (1991).

[7] N. Vinh Mau and A. Bouyssy, Nucl. Phys. A **257**, 189 (1976).

[8] F. Osterfeld, J. Wambach, and V. A. Madsen, Phys. Rev. C **23**, 179 (1981); V. A. Madsen and F. Osterfeld, *ibid.* **39**, 1215 (1989).

[9] J. R. M. Annand, R. W. Finlay, and F. E. Dietrich, Nucl. Phys. A **443**, 249 (1985); R. W. Finlay, J. Wierzbicki, R. K. Das, and F. S. Dietrich, Phys. Rev. C **39**, 804 (1989).

[10] S. G. Cooper and R. S. Mackintosh, Phys. Rev. C **43**, 1001 (1991); R. S. Mackintosh and S. G. Cooper, in *Quantum Inversion Theory and Application*, Lecture Notes in Physics Vol. 427, edited by H. von Geramb (Springer, Berlin, 1994), p. 266.

[11] A. Csótó, R. G. Lovas, and A. T. Kruppa, Phys. Rev. Lett. **70**, 1389 (1993).

[12] S. G. Cooper, R. S. Mackintosh, and A. A. Ioannides, Nucl. Phys. A **472**, 101 (1987).

[13] A. M. Kobos and R. S. Mackintosh, J. Phys. G **5**, 97 (1979).

[14] H. Feshbach, Ann. Phys. (N.Y.) **5**, 357 (1958); **19**, 287 (1962).

[15] H. Feshbach, *Theoretical Nuclear Physics* (Wiley, New York, 1992).

[16] T. Kaneko, M. LeMere, and Y. C. Tang, Phys. Rev. C **44**, 1588 (1991); **45**, 2409 (1992); **46**, 298 (1992).

[17] R. S. Mackintosh and A. M. Kobos, Phys. Lett. **116B**, 95 (1982); S. G. Cooper and R. S. Mackintosh, Inverse Problems **5**, 707 (1989); "IMAGO User's Manual," Open University Report OUPD9201, 1992.

[18] H. Fiedeldey, Nucl. Phys. **77**, 149 (1966); A **96**, 463 (1967); A **115**, 97 (1968); M. Coz, L. G. Arnold, and A. D. MacKellar, Ann. Phys. (N.Y.) **58**, 504 (1970); **59**, 219 (1970).

[19] W. Bauhoff, H. V. von Geramb, and G. Palla, Phys. Rev. C **27**, 2466 (1983).

[20] D. Lukaszek, Ph.D. dissertation, University of Connecticut, 1994.

[21] N. Yamaguchi, S. Nagata, and T. Matsuda, Prog. Theor. Phys. **70**, 459 (1983).

[22] B. T. Kim and T. Udagawa, Phys. Rev. C **42**, 1147 (1990).

[23] B. Z. Georgiev and R. S. Mackintosh, Phys. Lett. **73B**, 250 (1978).

[24] M. Reeves and L. W. Owen, J. Comput. Phys. **4**, 572 (1969).

[25] G. Rawitscher, Phys. Rev. C **25**, 2196 (1982); G. Delic and G. H. Rawitscher, J. Comput. Phys. **57**, 188 (1985); G. H. Rawitscher, *ibid.* **94**, 81 (1991).

[26] J. S. Petler, M. S. Islam, R. W. Finlay, and F. S. Dietrich, Phys. Rev. C **32**, 673 (1985).

[27] N. Austern, Phys. Rev. **137**, B752 (1965).

[28] R. S. Mackintosh and L. A. Cordero-L, Phys. Lett. **68B**, 213 (1977); A. M. Kobos and R. S. Mackintosh, J. Phys. G **5**, 97 (1979).

[29] H. Fiedeldey, R. Lipperheide, G. H. Rawitscher, and S. A. Sofianos, Phys. Rev. C **45**, 2885 (1992).